HAL
open science

Torsional-rotational spectrum of doubly deuterated dimethyl ether (CH3OCHD2)

C. Richard, J. K. Jørgensen, L. Margulès, R. A. Motiyenko, J.-C. Guillemin, P. Groner

To cite this version:

C. Richard, J. K. Jørgensen, L. Margulès, R. A. Motiyenko, J.-C. Guillemin, et al.. Torsional-rotational spectrum of doubly deuterated dimethyl ether (CH3OCHD2). Astronomy and Astrophysics - A&A, 2021, 651, pp.A120. 10.1051/0004-6361/202141282 . hal-03306201

HAL Id: hal-03306201

https://hal.science/hal-03306201v1

Submitted on 28 Jul 2021

HAL is a multi-disciplinary open access archive for the deposit and dissemination of scientific research documents, whether they are published or not. The documents may come from teaching and research institutions in France or abroad, or from public or private research centers.

L'archive ouverte pluridisciplinaire **HAL**, est destinée au dépôt et à la diffusion de documents scientifiques de niveau recherche, publiés ou non, émanant des établissements d'enseignement et de recherche français ou étrangers, des laboratoires publics ou privés.

A&A 651, A120 (2021)
https://doi.org/10.1051/0004-6361/202141282
© C. Richard et al. 2021

Astronomy & Astrophysics

Torsional-rotational spectrum of doubly deuterated dimethyl ether (CH_3OCHD_2)

First ALMA detection in the interstellar medium★

C. Richard[1], J. K. Jørgensen[2], L. Margulès[3], R. A. Motiyenko[3], J.-C. Guillemin[4], and P. Groner[5]

[1] Laboratoire Interdisciplinaire Carnot de Bourgogne, UMR 6303 CNRS - Université Bourgogne Franche-Comté, 9 Av. A. Savary, BP 47870, 21078 Dijon Cedex, France
e-mail: cyril.richard@u-bourgogne.fr
[2] Niels Bohr institute, University of Copenhagen, Øster Voldgade 5-7, 1350 Copenhagen K., Denmark
[3] Univ. Lille, CNRS, UMR 8523 - PhLAM - Physique des Lasers Atomes et Molécules, 59000 Lille, France
[4] Univ Rennes, Ecole Nationale Supérieure de Chimie de Rennes, CNRS, IRCR-UMR 6226, 35000 Rennes, France
[5] Department of Chemistry, University of Missouri-Kansas City, Kansas City, MO 64110-2499, USA

Received 10 May 2021 / Accepted 14 June 2021

ABSTRACT

Context. In 2013, we published the first rotational analysis and detection of mono-deuterated dimethyl ether in the solar-type protostar IRAS 16293-2422 with the IRAM 30 m telescope. Dimethyl ether is one of the most abundant complex organic molecules in star-forming regions, and its D-to-H (D/H) ratios are important to understand its chemistry and trace the source history.
Aims. We present the first analysis of doubly deuterated dimethyl ether (methoxy-d_2-methane, 1,1-dideuteromethylether) in its ground-vibrational state, based on an effective Hamiltonian for an asymmetric rotor molecule with internal rotors. The analysis covers the frequency range 0.15–1.5 THz.
Methods. The laboratory rotational spectrum of this species was measured between 150 and 1500 GHz with Lille's submillimeter spectrometer. For the astronomical detection, we used the Atacama Large Millimeter/submillimeter Array observations from the Protostellar Interferometric Line Survey.
Results. New sets of spectroscopic parameters have been determined by a least squares fit with the ERHAM code for both symmetric and asymmetric conformers. As for the mono-deuterated species, these parameters have permitted the first identification in space of both conformers of a doubly deuterated dimethyl ether via detection near the B component of the Class 0 protostar IRAS 16293-2422.

Key words. molecular data – submillimeter: ISM – ISM: molecules – astrochemistry

1. Introduction

By May 2021, around 220 molecules have been detected in the interstellar medium (ISM) or circumstellar shells[1]. Complex organic molecules (COMs) are ubiquitous in the ISM, especially close to the forming low-mass stars where the dust temperature is high enough to sublimate ice. With its nine atoms, dimethyl ether (CH_3—O—CH_3, hereafter DME), which was first detected in the ISM by Snyder et al. (1974), is a large COM of relevance for astrochemistry and one of the main COMs present in these warm and dense inner regions of the envelopes of Class 0 protostars, the so-called hot corinos (Ceccarelli et al. 2004). With the high sensitivity offered by new observations from the Atacama Large Millimeter/submillimeter Array (ALMA), new opportunities are opened up for characterizing the abundances of these COMs systematically (see, e.g., Jørgensen et al. 2020, for a recent review).

One of the characteristics of the molecules present in the warm gas in hot corinos is their high degree of deuteration. Although, the cosmic deuterium abundance relative to hydrogen is $1.5-2.0\times10^{-5}$ (e.g., Linsky 2003; Prodanović et al. 2010), the abundances of deuterated COMs relative to their non-deuterated counterparts are found to be much higher, up to ≈ 10% or more in some cases (e.g., Parise et al. 2006; Jørgensen et al. 2018). These enhancements are thought to be a result of the exothermic reaction $H_3^+ + HD \leftrightarrows H_2D^+ + H_2 + \Delta E$ that in gas at low temperatures enhances H_2D^+ relative to H_3^+. This effect is even more pronounced when one considers the multiple-deuterated variants, which for several species (e.g., D_2CO, Persson et al. 2018; CHD_2OHCHO, Manigand et al. 2019, D_2O, Jensen et al. 2021) are even further enhanced compared to the relative abundances of the mono- and non-deuterated species, possibly related to the buildup of the ice mantles where these species are formed.

Dimethyl ether is an interesting target species to extend these studies due to its structure and high abundance. The detection of the mono-deuterated form of CH_3OCH_3 toward the Class 0 protostellar system IRAS 16293-2422 was first reported by Richard et al. (2013) based on the detection of 20 lines of its symmetric and asymmetric conformers. Through ALMA observations, Jørgensen et al. (2018) determined the D/H ratio for these conformers (corrected for the number of equivalent hydrogen atoms)

★ Full Tables A.1, A.2, B.1, and B.2, which respectively give the measured (in laboratory) and predicted frequencies, are only available at the CDS via anonymous ftp to cdsarc.u-strasbg.fr (130.79.128.5) or via http://cdsarc.u-strasbg.fr/viz-bin/cat/J/A+A/651/A120

[1] https://cdms.astro.uni-koeln.de/classic/molecules

Open Access article, published by EDP Sciences, under the terms of the Creative Commons Attribution License (https://creativecommons.org/licenses/by/4.0), which permits unrestricted use, distribution, and reproduction in any medium, provided the original work is properly cited.

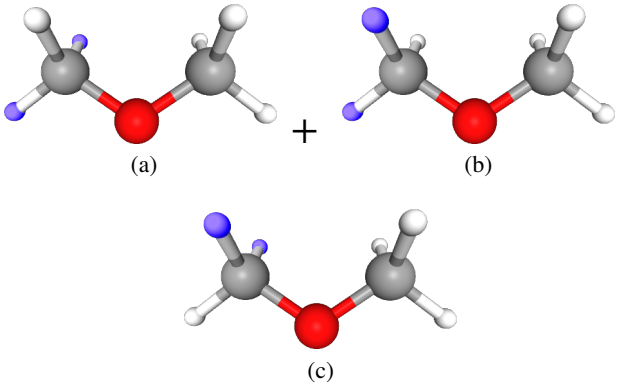

Fig. 1. Representation of the doubly deuterated DME with hydrogen atoms that are pictured in white and deuterium in blue. Figures 1a and 1b show the two possible configurations for the asymmetric conformer, while Fig. 1c illustrates the symmetric one.

of about 3% toward one component in this source, IRAS 16293B. With the high overall column density of DME toward this source, its D/H ratio, and potential enhancement of the doubly deuterated species, this would be a natural place to test new spectroscopic predictions for the multi-deuterated variants.

As we already have detailed in the analysis of the mono-deuterated species, DME is a near-prolate asymmetric top (Ray's asymmetry parameter $\kappa = -0.922$) with only a b-dipole moment component, $\mu_b = 1.302$ D (Blukis et al. 1963). The partial deuteration of one CH_3 group leads to two possible configurations. Figure 1 illustrates the molecule studied in this paper, the doubly deuterated DME (2D-DME), also called methoxy-d_2-methane in order to avoid confusion as to the locations of D atoms. The asymmetric conformation is identified when one of the deuteriums is located on the C–O–C plane and the second is located in one of the other two locations. Therefore this conformer has two equivalent configurations (a) and (b) in Fig. 1, with a possible tunneling effect between them as detected for some lines of the mono-deuterated species (Richard et al. 2013). When both deuterium atoms are outside of the C–O–C plane, the conformation is called symmetric as it has a symmetry plane and thus belongs to the C_s symmetry point group. In this study, the two conformations of 2D-DME were considered as two independent asymmetric top molecules each with a single unsubstituted CH_3 internal rotor. The independence in the treatment of their rotational spectra consisted in ignoring the possible effects of tunneling between two equivalent configurations of the asymmetric conformation or between symmetric and asymmetric conformations. This paper presents the first analysis of the 2D-DME from 0.15 to 1.5 THz (or 150 to 1500 GHz) and reports its detection toward the B component toward IRAS 16293-2422.

2. Experimental details

2.1. Preparation of the doubly deuterated DME (methoxy-d_2-methane, 1,1-dideuteromethylether)

Potassium methoxide and p-toluenesulfonyl chloride were purchased from Sigma-Aldrich. Methan-d_2-ol was purchased from Eurisotop.

Doubly deuterated dimethyl ether was synthesized by the reaction of potassium methoxide with 4-methylbenzenesulfonic acid, methyl-d_2 ester. The latter was prepared as previously reported for the trideutero derivative, but using methan-d_2-ol as alcohol (Yamamoto et al. 2016). In a three-necked flask under nitrogen and connected to a trap immersed in a cold bath of dry ice, potassium methoxide (5.6 g, 80 mmol) and dry DMSO (30 mL) were introduced. The mixture was heated to 60 °C and 4-methylbenzenesulfonic acid, methyl–d_2 ester (8.2 g, 40 mmol) in dry DMSO (20 mL) was added dropwise. The doubly deuterated DME was distilled off as it formed and condensed in the cold trap. At the end of the addition, the mixture was heated for 1 h at 80 °C. The trap was then closed with stopcocks. The yield was 1.0 g, thus 53%.

2.2. Nuclear magnetic resonance (NMR) of the doubly deuterated DME

^{1}H NMR ($CDCl_3$, 400 MHz) δ 3.18 (quint, 1H, $^2J_{HD}$ = 1.6 Hz, CHD_2); 3.23 (s, 3H, CH_3). ^{13}C NMR ($CDCl_3$, 100 MHz) δ 59.5 (quint, $^1J_{CD}$ = 21.6 Hz, $^1J_{CH}$ = 139.5 Hz (d), CHD_2); 60.1 (q, $^1J_{CH}$ = 140.4 Hz, CH_3).

2.3. Lille THz spectrometer

The absorption spectra were measured between 150 and 1500 GHz using the Lille spectrometer (Zakharenko et al. 2015). The absorption cell was a stainless steel tube (6 cm in diameter and 220 cm in length). The measurements were performed at typical pressures of 35–60 Pa at room temperature. The different frequency ranges were covered with various active and passive frequency multipliers with the Agilent synthesizer (12.5–18.6 GHz) used as the primary signal source. To increase the sensitivity of the spectrometer, frequency modulation at 20.5 kHz of the reference source and lock-in detection were used. The demodulation of the detected signal may be performed either at $1f$ or $2f$, but $2f$ demodulation is preferred because of the simpler presentation of the observed spectrum in this case. Absorption signals were detected by an InSb liquid He-cooled bolometer (QMC Instruments Ltd.). Estimated uncertainties for measured line frequencies are 30, 50, and 100 kHz depending on the observed signal-to-noise ratio (S/N) and the frequency range.

3. Spectral analysis

Similarly to the mono-deuterated species, the spectrum of the 2D-DME shows a very dense structure which is caused by the lines of the ground and the lowest excited vibrational states of symmetric and asymmetric conformations (See Fig 2). In addition, due to internal rotation of the unsubstituted methyl top, each rotational level of the two conformations is split into A and E symmetry components of the C_{3v} symmetry point group. Despite a relatively high barrier to internal rotation of $V_3 \approx 900$ cm^{-1} (see Table 1), the $A - E$ splittings of rotational transitions were resolved for the majority of the ground state lines of the 2D-DME adding thus more complexity to the measured spectra. To treat the internal rotation, we used the ERHAM code (Groner 1997, 2012). The model used in the code refers to the so-called combined axes methods. It combines the rho-axis system in which the molecular Hamiltonian is set up, and the principal axes system to which the Hamiltonian is transformed. In the rho-axis system, the molecular internal z axis is set parallel to the ρ vector whose coordinates are calculated using the following expression:

$$\rho_g = \frac{\lambda_g I_\alpha}{I_g}, \ (g = x, y, z), \tag{1}$$

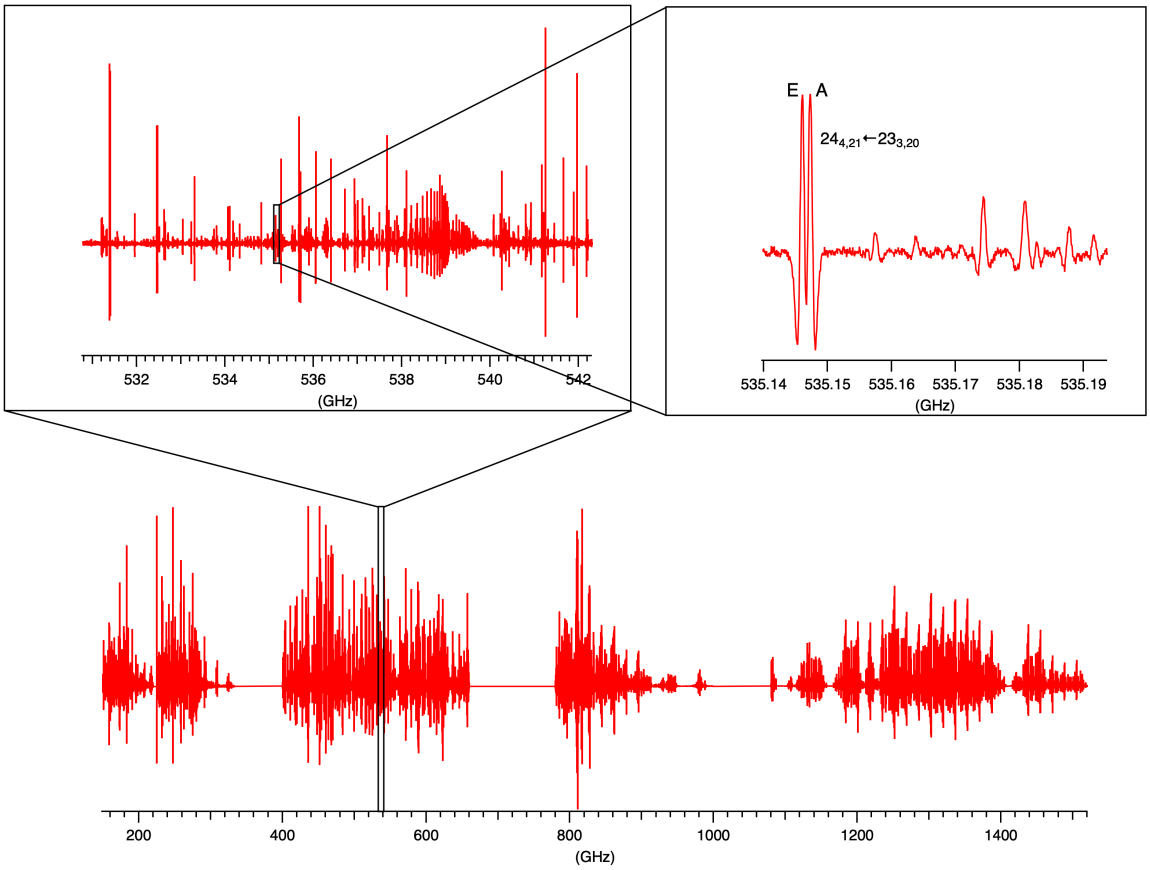

Fig. 2. Spectrum of doubly deuterated DME recorded in Lille. *Lower panel*: overall spectrum with a frequency range up to 1.5 THz. A zoom to some analyzed blended rotational transitions of the symmetric conformer is shown in the upper right corner.

where λ_g represents the direction cosines of the internal rotation axis of the top in the principal axis system, I_g represents the principal inertia moments, and I_α is the inertia moment of the methyl top. The magnitude of the rho vector represents the coupling between internal rotation of the methyl top and overall rotation of the molecular frame. For the two conformations of 2D-DME, the rho values are relatively high (see Table 1). They represent an intermediate case of the torsion-rotation coupling in the line between cis methyl formate, $HCOOCH_3$, $\rho = 0.08$ (Ilyushin et al. 2009), and acetaldehyde, $CH_3C(O)H$, $\rho = 0.3$ (Smirnov et al. 2014). For the latter two, strong torsion-rotation coupling, and medium height barriers to internal rotation significantly complicated the analysis and required the inclusion of many higher order terms into Hamiltonian. In the present analysis of the 2D-DME, a high barrier to internal rotation simplified the treatment, and in addition to pure rotational Hamiltonian only five terms were needed to describe a torsional-rotational interaction at close to experimental accuracy.

The symmetric conformation of 2D-DME has a symmetry plane and thus belongs to the C_s symmetry point group. Therefore, in the ERHAM code, the symmetry parameters ISCD is set to -1 and α, and the angle between the rho vector and *ab* principal axes plane is set to 0. On the other hand, the asymmetric conformation has a minimal symmetry and belongs to the C_1 group. Consequently, for the asymmetric conformation, ISCD = +1 and after various attempts to set a value to α, we decided to fix the parameter to 0 for the same reasons as discussed in the Sect. 4 of the mono-deuterated analysis (Richard et al. 2013).

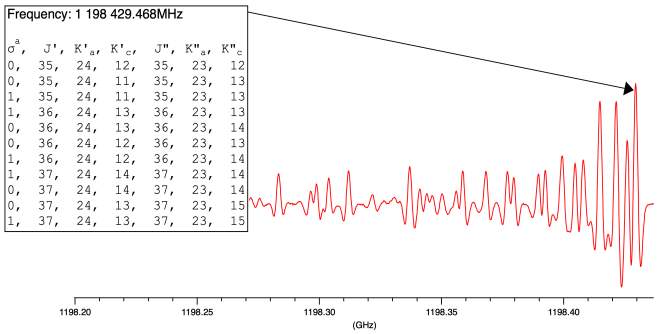

Fig. 3. Spectrum zoom showing series with $K' = 24$. All lines are extremely blended, making the analysis very difficult and uninteresting. Therefore they are not been included in the fit. $^{(a)}$symmetry number: $0(A)$, $1(E)$.

The analysis was started with a pattern recognition of a few $K_a = 0$ and $K_a = 1$ $^aR_{0,1}$ lines in order to produce a fit and a first prediction. Then, the fit was iteratively improved, releasing more parameters by adding new identified lines.

One difficulty encountered during the analysis was caused by several series of high K_a $^bQ_{1,-1}$ transitions. An example is given in Fig. 3 for the $K_a = 24$ series. In this case, the spectral lines in the band head represent a congestion of many rotational transitions with different J quantum numbers and different torsional symmetries. Such congestion has a strong influence on the spectral line shape. Taking the spectral congestion and the

Table 1. Spectroscopic constants of the ground-vibrational state of doubly deuterated DME for the two different conformers.

Parameters	Symmetric conformer	Asymmetric conformer
Pure Rotation		
A (MHz)	31 492.87567(43)	34 199.90529(31)
B (MHz)	9226.37143(19)	8976.84575(12)
C (MHz)	8256.93333(16)	7984.12140(11)
Δ_J (kHz)	8.18522(15)	7.001791(72)
Δ_{JK} (kHz)	−6.03171(74)	−12.80820(49)
Δ_K (kHz)	167.2067(20)	208.1287(14)
δ_J (kHz)	1.541683(51)	1.335158(25)
δ_K (kHz)	−31.8881(24)	−4.1331(15)
Φ_J (Hz)	0.007359(31)	0.003928(15)
Φ_{JK} (Hz)	0.1469(29)	0.0908(12)
Φ_{KJ} (Hz)	−2.5745(84)	−2.8404(39)
Φ_K (Hz)	5.8044(60)	6.8016(32)
ϕ_J (Hz)	0.003775(15)	0.001907(68)
ϕ_{JK} (Hz)	0.50088(97)	0.10031(62)
ϕ_K (Hz)	1.779(83)	2.857(41)
Tunneling terms		
ρ	0.17032(43)	0.19123(14)
β (deg)	10.935(47)	8.718(19)
α (deg)	0.0 [(a)]	0.0 [(b)]
ε_{10} (MHz)	−2.1814(73)	−2.4740(42)
$[A-(B+C)/2]_{q=1}$ (kHz)	0.443(65)	0.438(49)
$[(B-C)/4]_{q=1}$ (kHz)	0.0626(92)	0.0805(40)
V_3 [(c)] (10^2cm^{-1})	9.014(30)	9.044(15)
Lines fitted [(d)]	1451	2080
J(max), K_a(max)	88, 27	74, 25
$L_{\rm worst}$ [(e)]	−4.4	−4.8
n [(f)]	20	20
$\sigma_{\rm fit}$ [(g,f)] (MHz)	0.080	0.077
$\sigma_{\rm w}$ [(h)]	1.09	1.01

Notes. Numbers in parentheses are one standard deviation in the same units as the last digit. [(a)]By symmetry. [(b)]Assumed, see Sect. 4 in Richard et al. (2013). [(c)]Barrier height for rotation of the methyl group determined with the program BARRIER. See Sect. 4 for uncertainties regarding the computation. [(d)]Number of distinct lines in the fit. [(e)]$(o.-c.)$/error of the poorest fit line. [(f)]Number of free parameters used in the fit. [(g)]Standard deviation of the fit. [(h)]Weighted standard deviation of the fit.

second derivative spectrum into account, it leads to a significantly reduced line frequency measurement accuracy, typically three to ten times less accurate than usual. In the weighted least-squares fit implemented in the ERHAM code, the weight of each frequency is calculated to be reciprocal to the measurement accuracy squared. The influence of such highly congested lines would be ten to 100 times less important. Therefore, we decided to remove these congested lines from the final fit and to include only the lines from such a series that could be considered as isolated ones.

A total of 1451 lines with $J_{\rm max}$ = 71 and $K_{a,\rm max}$ = 27 and 2080 lines with $J_{\rm max}$ = 72 and $K_{a,\rm max}$ = 25 were assigned for symmetric and asymmetric conformers, respectively. For each conformer, a set of 15 pure rotational and five torsional-rotation parameters of the effective Hamiltonian implemented in the ERHAM code was needed to fit the observed molecular lines. The determined parameters are listed in Table 1. In the torsional-rotational part of the Hamiltonian, besides ρ, we determined the following parameters: β the angle between rho vector and principal axis a, ε_{10} the tunneling parameter representing the splitting between A and E symmetry sublevels, and two rotational constant tunneling parameters ($[A-(B+C)/2]_{q=1}$ and $[(B-C)/4]_{q=1}$).

4. Discussion

This study represents the first comprehensive characterization of the rotational spectrum of the two conformations of 2D-DME (CH_3OCHD_2) in the ground vibrational state, and in the frequency range up to 1.5 THz. Experimental measurements, partially given in the appendices in Tables A.1 and A.2, are available in their entirety in electronic form at the Centre de Données astronomiques de Strasbourg (CDS).

In the ERHAM code, the barrier to internal rotation is not calculated explicitly. Consequently, we used the program BARRIER which is derived from the program ASTOR described in Groner et al. (1986) that determines the potential barrier for a single simple internal rotor from torsional transitions or splittings. The ground state energy splitting between the A and E symmetry torsional substates, $\Delta E(E-A)$, was combined with the derived value of the internal rotation constant F to obtain an estimate of the potential barrier V_3 for both conformers. These values are the direct output of ERHAM. In particular, the internal rotation constants, F, is obtained by ERHAM from ρ, β, and the rotational constants. The F values determined in this study are 6.223 and 6.338 cm^{-1} for symmetric and asymmetric conformers, respectively. The determined V_3 values are given in Table 1. The estimated error of the V_3 barriers was derived with the assumption that the relative error of V_3 is the same as the relative errors of the $\Delta E(E-A)$ energy difference and the tunneling coefficient ε_{10}. We found an uncertainty of 3 and 1.5 cm^{-1} for the symmetric and asymmetric conformers, respectively. The determined barrier heights agree well with the results of the study of monodeuterated DME (Richard et al. 2013), and with earlier studies of parent DME (Durig et al. 1976; Lovas et al. 1979).

Under Doppler limited spectral resolution, we did not observe any additional splittings in the ground state rotational lines of the asymmetric conformation as it could be expected, owing to possible tunneling between its two equivalent configurations, and as it was previously observed for monodeuterated DME (Richard et al. 2013). It should be noted that for the latter, the tunneling splittings were barely resolved for a limited number of lines. The lack of additional tunneling splittings for the asymmetric conformer may be explained by the increased mass of the internal rotor which is composed of two deuteriums and one hydrogen for 2D-DME. Provided that the barrier height does not vary significantly under H to D isotopic substitution, the increased internal rotor mass reduces the tunneling probability and consequently the splitting between the two tunneling substates (compared to monodeuterated DME). In this case, one could also expect smaller and unresolvable splittings under the Doppler limit in the rotational spectra. The absence of resolved additional splittings as well as the weighted rms deviations of the fits close to 1 support our initial strategy to treat the two conformations independently as two asymmetric rotors each having a single methyl top.

Table 2. Rotational partition function for the symmetric and asymmetric conformers of doubly deuterated DME in the ground vibrational state computed for nine different temperatures.

Temperature	2.275 K	5 K	9.375 K	18.75 K	37.5 K	75 K	150 K	225 K	300 K
					Symmetric conformer				
Approx. [(a)]	94.481	307.843	790.372	2235.509	6322.974	17 884.072	50 583.794	92 928.364	143 072.576
Total	100.006	315.891	801.356	2251.224	6346.528	17 925.034	50 684.990	93 140.580	143 460.262
Ratio	1.058	1.026	1.014	1.007	1.004	1.002	1.002	1.002	1.003
					Asymmetric conformer				
Approx. [(a)]	186.947	609.120	1563.884	4423.333	12 511.074	35 386.660	100 088.590	183 874.482	283 093.284
Total	197.606	624.644	1585.062	4453.594	12 556.198	35 463.956	100 274.098	184 257.132	283 786.136
Ratio	1.057	1.025	1.013	1.007	1.004	1.002	1.002	1.002	1.002

Notes. [(a)]These values were computed with the rigid asymmetric rotor approximation.

5. Predictions

Thanks to the new set of spectroscopic parameters given in Table 1 and using the ERHAM software in its "ERHAM V16g-R3" version (downloaded on the PROSPE website (Kisiel 2001)), we calculated predictions in the JPL catalog format (Pickett 1991) up to 1.5 THz. Two short examples are provided in Tables B.1 and B.2 from 150.1 to 153.5 GHz. The complete tables are available in their entirety in electronic form at the CDS.

Numerical values of overall partition functions were computed at nine different temperatures using the ERHAM output and are reported in the Table 2. A good approximation of these values can be obtained from the simple rigid asymmetric rotor approximation (Townes & Schawlow 1975) and is expressed in the following formula:

$$g_n \sum_J (2J+1) e^{-\frac{E_{\rm rot}(J,K)}{kT}} = g_n \sqrt{\frac{\pi}{ABC}\left(\frac{k}{h}\right)^3} T^{3/2}. \quad (2)$$

In Eq. (2), the degeneracy factor g_n is equal to 1 for the symmetric conformation and 2 for the asymmetric one since the latter has two equivalent configurations and each energy level is split into two sublevels. We thus obtain $27.53433T^{3/2}$ for the symmetric conformer and $54.48133T^{3/2}$ for the asymmetric one. These values have also been listed in the Table 2 for comparison purposes. However, only the results from the fit, which are highlighted in bold, were used to derive column densities.

6. Astronomical search for CH_3OCHD_2

As an application of the new spectroscopy, we searched for the two conformers of CH_3OCHD_2 in ALMA observations from the Protostellar Interferometric Line Survey, (PILS; Jørgensen et al. 2016). The PILS program is an unbiased molecular line survey of the protostellar system IRAS 16293-2422 with ALMA (project id: 2013.1.00278.S; PI: Jes Jørgensen). PILS covers a continuous frequency range from 329.1 to 362.9 GHz of the main atmospheric window in ALMA's Band 7. The spectral resolution over this full range is ≈0.2 km s^{-1} and the sensitivity ≈5 mJy beam^{-1} km s^{-1} with an angular resolution of 0.5″.

The advantage of looking for the deuterated species toward IRAS 16293-2422 is that it shows high D/H ratios for many organic molecules compared to, in particular, high-mass star forming regions otherwise targeted in studies of complex organic chemistry (e.g., Jørgensen et al. 2020, and references therein). For example, it was toward this source that a number of multiple deuterated species were identified for the first time (e.g., Loinard et al. 2000; Parise et al. 2002, 2003; Manigand et al. 2019) and recently the PILS survey has provided a comprehensive inventory of the deuterated content of the warm complex organic molecules close to the protostar (Jørgensen et al. 2018; Persson et al. 2018; Manigand et al. 2020).

To look for CH_3OCHD_2, here, we targeted a position offset by 0.5″ to the southwest from the "B" component of the system (IRAS16293B) – also the target of a number of the previous PILS papers. The advantage of searching at that position is that the lines are narrow (≈1 km s^{-1}) and the opacity of both the main lines of the dust continuum is limited. This enables easy assignments of individual transitions without problems with line overlaps and absorption.

At the targeted scales, the densities should be high enough for the excitation of the molecules to occur under local thermodynamic equilibrium (LTE) conditions. We consequently used synthetic spectra calculated under this assumption to identify the lines of CH_3OCHD_2 within the PILS range and used them to constrain their column density. The synthetic spectrum method is preferred over classical rotation diagrams, for example, as it immediately makes it possible both to search for good matches in the data and to show if lines are predicted at frequencies where no emission is seen. In particular, confirming the presence of rare species to demonstrate that the latter is not the case is equally important in finding good assigned matches. Also, this method makes it possible to predict the profiles for partially blended lines and also to look for overlaps with previously identified species.

Under the LTE assumption, the line profiles are calculated assuming Gaussian line profiles with constant LSR velocity offsets and line widths. Also, the extent of the source emission (and consequently beam filling factor) is kept constant. For these parameters, we adopted the same values as for the single-deuterated variants and most other species in the PILS range – a LSR velocity of 2.6 km s^{-1}, a line width (FWHM) of 1 km s^{-1}, and source size of 0.5″ (assumed as a Gaussian distribution). The choices of the LSR velocity and line width can be tested directly when comparing to the observed spectra. The assumed source size mainly affects the results when optically thick lines are considered: in the case of optically thin emission and when species that are thought to be co-existent in the gas, it does not affect the derived relative abundances.

With these choices of fixed parameters, what remains to be fitted are the column densities of the species and their excitation

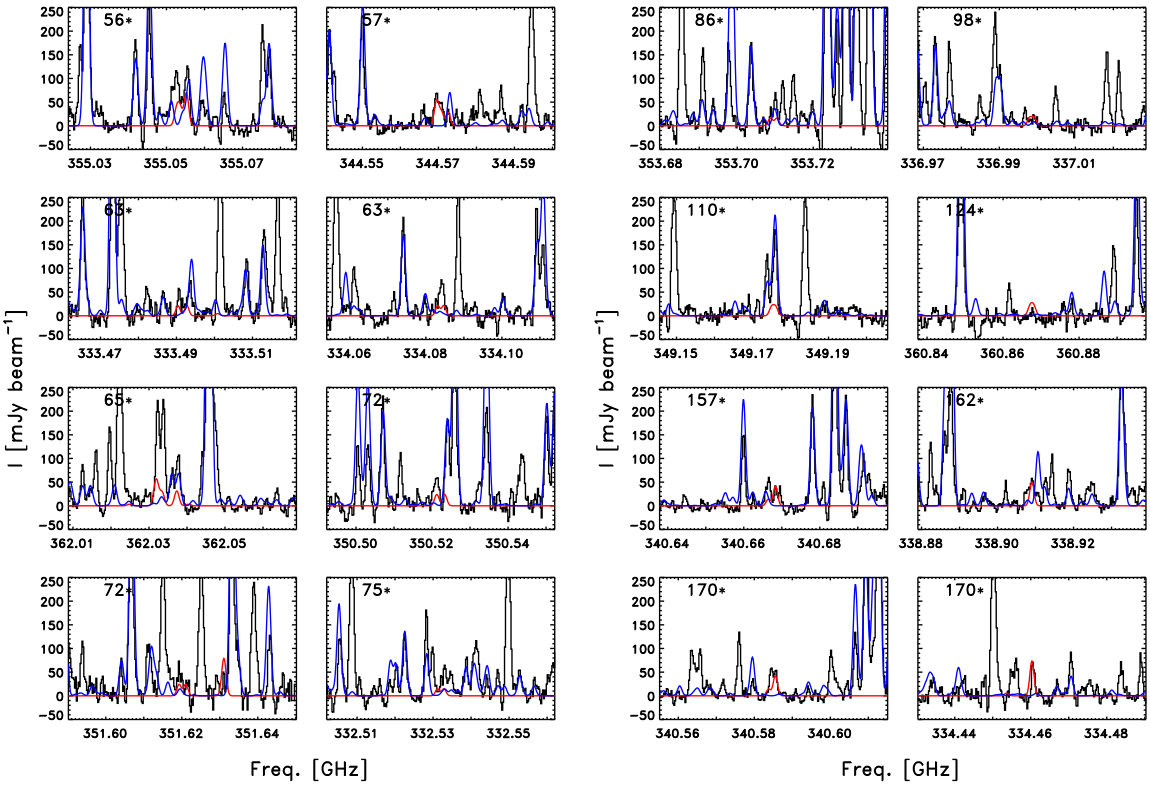

(a) (b)

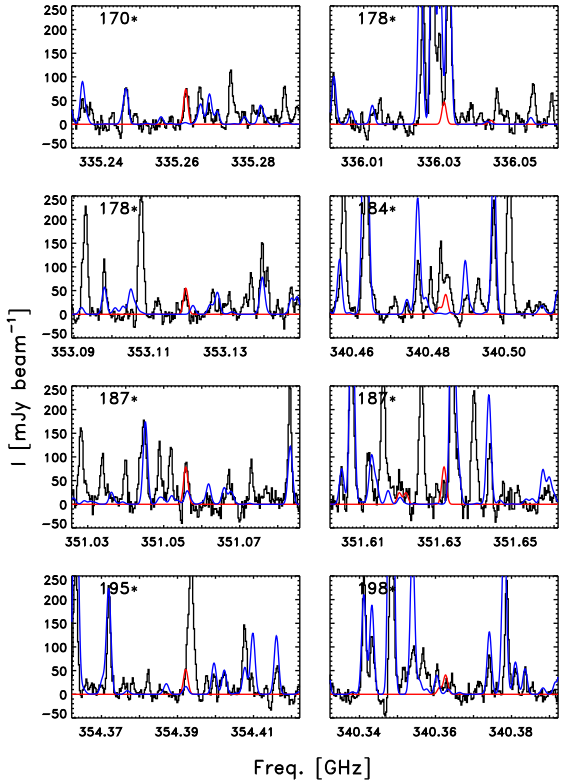

(c)

Fig. 4. Spectra for the 24 transitions of the symmetric conformer of CH_3OCHD_2 predicted to be the strongest given the derived excitation temperature and column density. In the panels, the red line shows the fit to the CH_3OCHD_2 transition while the blue lines show the predictions for of all other species identified as part of the PILS survey (see, e.g., Drozdovskaya et al. 2019; Manigand et al. 2020, and references therein).

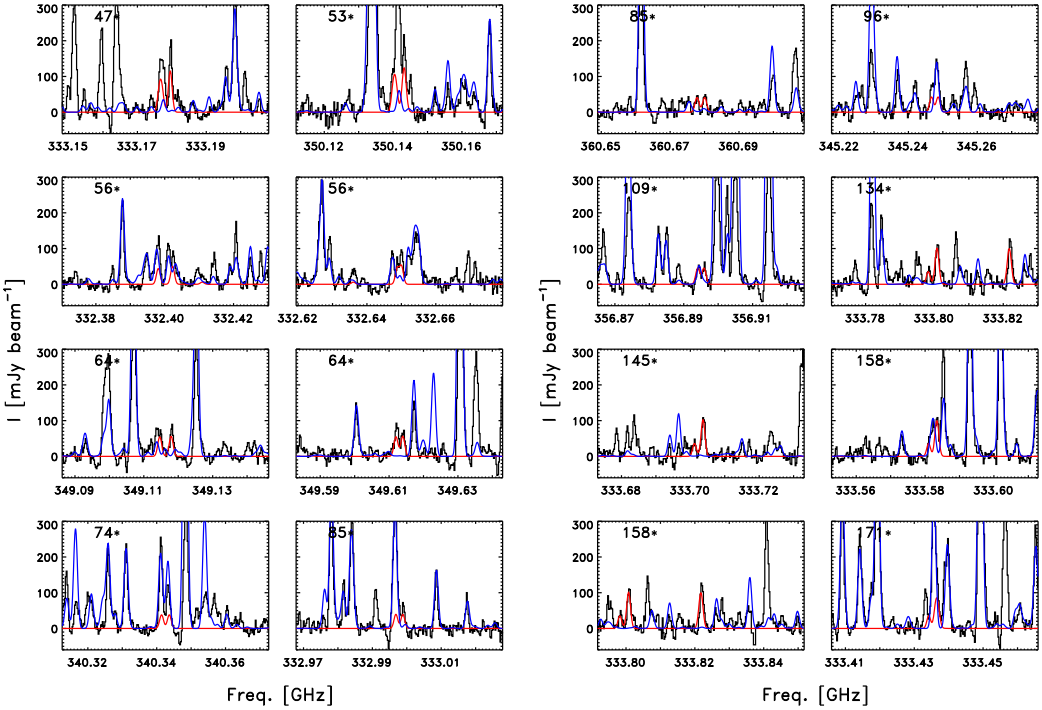

(a) (b)

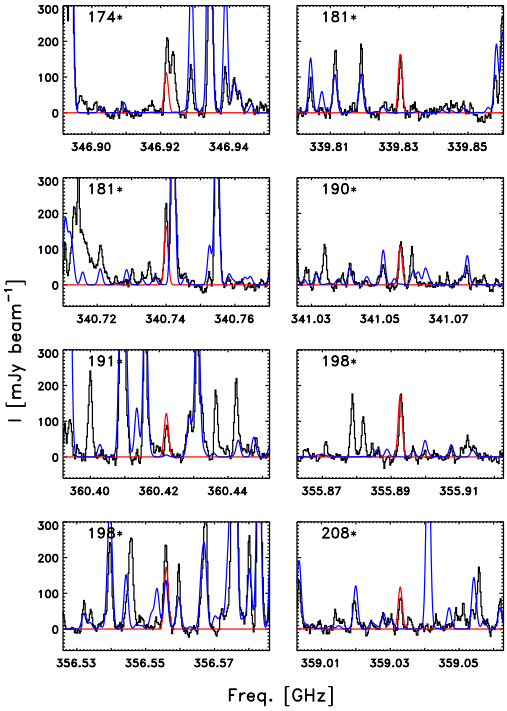

(c)

Fig. 5. Spectra for the 24 transitions of the asymmetric conformer of CH_3OCHD_2 predicted to be the strongest given the derived excitation temperature and column density.

temperature. For the latter, we adopted a temperature of 125 K of the non- and singly-deuterated variants of dimethylether, again under the assumption that the doubly deuterated variants are present in the same gas. We then performed χ^2-fitting to the reasonably isolated lines to constrain the column densities of the symmetric and asymmetric conformers separately.

Figures 4 and 5 show the 24 lines predicted in this manner to be the strongest for the asymmetric and symmetric conformers. For the two species, good fits can be seen for about 20 transitions – a number of which are well-isolated with peak intensities of up to about 200 mJy beam^{-1}. The derived column densities are 6.1×10^{15} cm^{-2} for the asymmetric conformers

and 2.7×10^{15} cm^{-2} for the symmetric conformers. A priori, one would expect a factor 2 difference between the two due to the symmetry that occurs when two deuterium atoms replace two of the three hydrogen atoms in a CH_3-group of dimethyl ether. The factor 2.3 we derived when fitting the two conformers independently is consequently an additional verification of the assignment of the two conformers.

Taken together, the derived column densities imply a ratio between the column densities of the doubly to mono deuterated forms, $N(CH_3OCHD_2)/N(CH_3OCH_2D)$ of 15–20% for the two conformers. These imply D/H ratios that are about a factor of 5 higher than those inferred from the singly to non deuterated variants once corrected for the number of equivalent hydrogen atoms (e.g., Appendix B of Manigand et al. 2019). The trend of strong enhancements of the multi-deuterated variants also seen for other COMs thus also holds for DME, and they provide additional constraints on their formation during the cold phases of star formation.

7. Conclusion

Here, we have presented a complete high-resolution study of the doubly deuterated dimethylether over a decade in the frequency range 150–1500 GHz (0.15–1.5 THz) in its two conformations, symmetric and asymmetric. We were able to determine an accurate set of spectroscopic parameters that allowed us to reproduce measurements with a standard deviation better than 80 kHz. Thanks to these frequency predictions, both conformers have been detected near the "B" component of the protostellar system IRAS 16293-2422. The doubly deuterated species is found to be enhanced above the D/H ratio inferred from the mono-to-singly deuterated variants at a level similar to other organic molecules. These enhancements make CH_3OCH_3 an interesting target for further spectroscopic studies of other multiple deuterated variants, which in turn may shed light on the formation of this complex organic during the cold pre- and protostellar stages.

Acknowledgements. This work has been supported by the "Programme National Physique et Chimie du Milieu Interstellaire" (PCMI) of CNRS/INSU with INC/INP co-funded by CEA and CNES. This project has received financial support from the CNRS through the MITI interdisciplinary programs. J.C.G. thanks the Centre National d'Etudes Spatiales (CNES) for a grant. The research of J.K.J is supported by the Independent Research Fund Denmark (grant number 0135-00123B).

References

Blukis, U., Kasai, P. H., & Myers, R. J. 1963, J. Chem. Phys., 38, 2753
Ceccarelli, C., Johnstone, D., Adams, F., et al. 2004, ASP Conf. 323, 195
Drozdovskaya, M. N., van Dishoeck, E. F., Rubin, M., Jørgensen, J. K., & Altwegg, K. 2019, MNRAS, 490, 50
Durig, J., Li, Y., & Groner, P. 1976, J. Mol. Spectrosc, 62, 159
Groner, P. 1997, J. Chem. Phys., 107, 4483
Groner, P. 2012, J. Mol. Spectrosc., 278, 52
Groner, P., Johnson, R., & Durig, J. 1986, J. Mol. Struct., 142, 363
Ilyushin, V., Kryvda, A., & Alekseev, E. 2009, J. Mol. Spectrosc, 255, 32
Jensen, S. S., Jørgensen, J. K., Kristensen, L. E., et al. 2021, A&A, 650, A172
Jørgensen, J., Van der Wiel, M., Coutens, A., et al. 2016, A&A, 595, A117
Jørgensen, J. K., Müller, H. S. P., Calcutt, H., et al. 2018, A&A, 620, A170
Jørgensen, J. K., Belloche, A., & Garrod, R. T. 2020, ARA&A, 58, 727
Kisiel, Z. 2001, in Spectroscopy from Space (Berlin: Springer) 91
Linsky, J. L. 2003, in Solar System History from Isotopic Signatures of Volatile Elements, eds. R. Kallenbach, T. Encrenaz, J. Geiss, K. Mauersberger, T. Owen, & F. Robert (Berlin: Springer), 49
Loinard, L., Castets, A., Ceccarelli, C., et al. 2000, A&A, 359, 1169
Lovas, F., Lutz, H., & Dreizler, H. 1979, J. Phys. Chem. Ref. Data, 8, 1051
Manigand, S., Calcutt, H., Jørgensen, J. K., et al. 2019, A&A, 623, A69
Manigand, S., Jørgensen, J. K., Calcutt, H., et al. 2020, A&A, 635, A48
Parise, B., Ceccarelli, C., Tielens, A. G. G. M., et al. 2002, A&A, 393, L49
Parise, B., Simon, T., Caux, E., et al. 2003, A&A, 410, 897
Parise, B., Ceccarelli, C., Tielens, A. G. G. M., et al. 2006, A&A, 453, 949
Persson, M. V., Jørgensen, J. K., Müller, H. S. P., et al. 2018, A&A, 610, A54
Pickett, H. M. 1991, J. Mol. Spectrosc., 148, 371
Prodanović, T., Steigman, G., & Fields, B. D. 2010, MNRAS, 406, 1108
Richard, C., Margulès, L., Caux, E., et al. 2013, A&A, 552, A117
Smirnov, I., Alekseev, E., Ilyushin, V., et al. 2014, J. Mol. Spectrosc., 295, 44
Snyder, L., Buhl, D., Schwartz, P., et al. 1974, ApJ, 191, L79
Townes, C. H., & Schawlow, A. L. 1975, Microwave Spectroscopy, ed. N. Y. D. P. inc. (North Chelmsford: Courier Corporation)
Yamamoto, C., Takamatsu, K., Hirano, K., & Miura, M. 2016, J. Org. Chem., 81, 7675
Zakharenko, O., Motiyenko, R. A., Margulès, L., & Huet, T. R. 2015, J. Mol. Spectrosc, 317, 41

Appendix A: Experimental frequencies

Table A.1. Experimental frequencies measured in laboratory up to 1.5 THz for the symmetric conformer.

σ [(a)]	J'	K'_a	K'_c	J''	K''_a	K''_c	Frequency (MHz)	Uncertainty (MHz)	o.-c. (MHz)
...									
1	13	4	9	13	3	10	154 472.280	0.099	0.0540
0	13	4	9	13	3	10	154 473.864	0.099	0.0236
1	20	3	18	20	2	19	154 580.928	0.099	–0.0216
0	20	3	18	20	2	19	154 582.476	0.099	–0.0186
1	12	4	8	12	3	9	155 928.264	0.099	0.0032
0	12	4	8	12	3	9	155 929.956	0.099	0.0344
1	11	4	7	11	3	8	157 006.536	0.099	0.0627
0	11	4	7	11	3	8	157 008.156	0.099	0.0303
1	10	4	6	10	3	7	157 779.384	0.099	0.0408
0	10	4	6	10	3	7	157 780.896	0.099	0.0283
0	23	5	19	22	6	16	157 954.344	0.099	0.0286
1	23	5	19	22	6	16	157 955.208	0.099	0.0140
1	9	4	5	9	3	6	158 315.460	0.099	0.0267
0	9	4	5	9	3	6	158 316.576	0.099	0.0247
0	8	4	4	8	3	5	158 674.920	0.099	–0.0426
...									

Notes. [(a)]Symmetry number: 0(A), 1(E).

Table A.2. Experimental frequencies measured in laboratory up to 1.5 THz for the asymmetric conformer.

σ [(a)]	J'	K'_a	K'_c	J''	K''_a	K''_c	Frequency (MHz)	Uncertainty (MHz)	o.-c. (MHz)
...									
1	28	3	25	28	2	26	150 936.099	0.050	0.0201
0	28	3	25	28	2	26	150 937.072	0.050	–0.0012
1	17	3	15	17	2	16	152 080.811	0.050	0.0429
0	17	3	15	17	2	16	152 082.764	0.050	0.0257
1	33	4	29	33	3	30	152 137.688	0.050	0.0841
1	23	2	21	23	1	22	152 153.268	0.050	–0.0116
0	23	2	21	23	1	22	152 154.840	0.050	–0.0291
0	20	3	18	19	4	15	152 639.222	0.050	–0.0005
1	20	3	18	19	4	15	152 640.886	0.050	–0.0189
1	20	4	16	20	3	17	153 413.952	0.099	0.0247
0	20	4	16	20	3	17	153 415.500	0.099	0.0270
1	17	2	16	17	1	17	155 133.960	0.099	0.0193
0	17	2	16	17	1	17	155 136.336	0.099	0.0180
0	10	0	10	9	1	9	155 368.536	0.099	0.0722
1	10	0	10	9	1	9	155 368.536	0.099	–0.1006
...									

Notes. [(a)]Symmetry number: 0(A), 1(E).

Appendix B: Predicted frequencies

Table B.1. Predicted transition frequencies of doubly deuterated DME in the ground-vibrational state for the symmetric conformer.

σ [(a)]	J'	K'_a	K'_c	J''	K''_a	K''_c	Frequency (MHz)	Uncertainty (MHz)	Spin weight	S	E (cm^{-1})
1	15	4	11	15	3	12	150 168.493	0.004	4	7.9007	82.305
0	15	4	11	15	3	12	150 169.934	0.005	4	7.9010	82.305
0	28	15	14	29	14	15	150 188.926	0.010	4	0.0775	407.265
0	28	15	13	29	14	16	150 188.926	0.010	4	0.0775	407.265
1	28	15	14	29	14	16	150 189.636	0.011	4	0.0775	407.265
1	28	15	13	29	14	15	150 189.708	0.009	4	0.0775	407.265
0	27	2	26	26	3	23	150 530.744	0.018	4	0.1022	220.054
1	27	2	26	26	3	23	150 533.598	0.018	4	0.1022	220.054
1	5	2	4	4	1	3	150 807.089	0.002	4	4.0124	11.780
0	5	2	4	4	1	3	150 808.179	0.003	4	4.0125	11.780
0	30	5	25	30	4	26	151 255.992	0.009	4	2.7557	291.944
1	30	5	25	30	4	26	151 256.456	0.007	4	2.7557	291.944
1	15	10	6	16	9	8	151 518.542	0.008	4	0.3512	145.838
0	15	10	6	16	9	7	151 519.578	0.009	4	0.3512	145.838
0	15	10	5	16	9	8	151 519.578	0.009	4	0.3512	145.838
...											

Notes. [(a)]Symmetry number: 0(A), 1(E).

Table B.2. Predicted transition frequencies of doubly deuterated DME in the ground-vibrational state for the asymmetric conformer.

σ [(a)]	J'	K'_a	K'_c	J''	K''_a	K''_c	Frequency (MHz)	Uncertainty (MHz)	Spin weight	S	E (cm^{-1})
1	28	3	25	28	2	26	150 936.079	0.005	4	3.5816	241.633
0	28	3	25	28	2	26	150 937.073	0.005	4	3.5817	241.633
0	25	5	20	24	6	19	151 482.629	0.004	4	1.0671	206.034
1	25	5	20	24	6	19	151 483.750	0.004	4	1.0669	206.034
1	17	3	15	17	2	16	152 080.768	0.003	4	7.3428	94.479
0	17	3	15	17	2	16	152 082.738	0.003	4	7.3430	94.479
1	33	4	29	33	3	30	152 137.604	0.004	4	2.0711	335.886
0	33	4	29	33	3	30	152 137.941	0.005	4	2.0711	335.886
1	23	2	21	23	1	22	152 153.280	0.006	4	4.8360	162.649
0	23	2	21	23	1	22	152 154.869	0.006	4	4.8361	162.649
0	20	3	18	19	4	15	152 639.222	0.004	4	1.7455	126.757
1	20	3	18	19	4	15	152 640.905	0.004	4	1.7455	126.757
1	20	4	16	20	3	17	153 413.927	0.003	4	7.5813	133.093
0	20	4	16	20	3	17	153 415.473	0.004	4	7.5814	133.093
1	11	4	8	12	1	11	153 421.035	0.007	4	0.0136	51.116
...											

Notes. [(a)]Symmetry number: 0(A), 1(E).